Received: 27 October 2021 | Revised: 3 January 2022 | Accepted: 22 January 2022

DOI: 10.1111/cyt.13106

ORIGINAL ARTICLE

WILEY

Deconvolution microscopy: A platform for rapid on-site evaluation of fine needle aspiration specimens that enables recovery of the sample

Haihui Liao[1] | Todd Sheridan[1] | Ediz Cosar[1] | Christopher Owens[2] | Tao Zuo[1] | Xiaofei Wang[1] | Ali Akalin[1] | Dina Kandil[1] | Karen Dresser[1] | Kevin Fogarty[1] | Karl Bellve[1] | Christina Baer[1] | Andrew Fischer[1]

[1]University of Massachusetts Medical School, Worcester, Massachusetts, USA

[2]Quest Diagnostics Inc., Malborough, Massachusetts, USA

Correspondence
Haihui Liao, University of Massachusetts Medical School, Worcester, Massachusetts, USA.
Email: haihui.liao@gmail.com

Abstract

Context: Rapid on-site evaluation (ROSE) optimises the performance of cytology, but requires skilled handling, and smearing can make the material unavailable for some ancillary tests. There is a need to facilitate ROSE without sacrificing part of the sample.

Objective: We evaluated the image quality of inexpensive deconvolution fluorescence microscopy for optically sectioning non-smeared fine needle aspiration (FNA) tissue fragments.

Design: A portion of residual material from 14 FNA samples was stained for 3 min in Hoechst 33342 and Sypro™ Red to label DNA and protein respectively, transferred to an imaging chamber, and imaged at 200× or 400× magnification at 1 micron intervals using a GE DeltaVision inverted fluorescence microscope. A deconvolution algorithm was applied to remove out-of-plane signal, and the resulting images were inverted and pseudocoloured to resemble H&E sections. Five cytopathologists blindly diagnosed 2 to 4 representative image stacks per case (total 70 evaluations), and later compared them to conventional epifluorescent images.

Results: Accurate definitive diagnoses were rendered in 45 (64%) of 70 total evaluations; equivocal diagnoses (atypical or suspicious) were made in 21 (30%) of the 70. There were two false positive and two false negative "definite" diagnoses in three cases (4/70; 6%). Cytopathologists preferred deconvolved images compared to raw images ($P < 0.01$). The imaged fragments were recovered and prepared into a ThinPrep or cell block without discernible alteration.

Conclusions: Deconvolution improves image quality of FNA fragments compared to epifluorescence, often allowing definitive diagnosis while enabling the ROSE material to be subsequently triaged.

KEYWORDS
deconvolution, fine-needle aspiration, fluorescence microscopy, optical sectioning, rapid on-site evaluation

1 | INTRODUCTION

The goal of rapid on-site evaluation (ROSE) is to ensure that a potentially invisible sample, obtained with micro-sized instruments, is adequate for full diagnostic work-up.[1] ROSE significantly reduces the non-diagnostic rate and the number of repeated procedures.[2-4] There is no standardised protocol for performing ROSE; however, smearing a portion of a sample from one pass is common to virtually all protocols. The smeared material is generally fixed by air-drying or alcohol, the slide is stained, and then examined by bright-field microscopy. The remaining specimen that was not smeared is saved in a needle rinse solution. Depending on the ROSE findings, additional samples (or portions of the additional samples) may need to be triaged for ancillary studies.

In the era of personalised medicine, ancillary studies are often required for the full diagnostic work-up needed to direct clinical management. Different ancillary studies have specific requirements for specimen collection, and the collection requirements vary for each laboratory. These ancillary studies may require triage of material into various potential fixatives for a cell block, triage into a physiological saline for flow cytometry or cytogenetics, triage into a nucleic acid-preserving solution for some molecular studies, or triage into a sterile vial for microbiology cultures. These various triages are mutually exclusive. While attempts have been made to allow the smear to be a source of material for molecular studies or immunocytochemistry[5] (after validation by each laboratory[6]), most laboratories use cell blocks as a source for these studies.[7,8]

Therefore, a significant limitation of ROSE is that the portion of the sample that has been smeared onto a slide for on-site microscopy often cannot be triaged for ancillary studies. As currently conducted, ROSE can only indirectly allow the cytologist to estimate the quantity or quality of the sample that has NOT been smeared and may be in the needle rinse. It is not uncommon for insufficient material to be present in the needle rinse solution for ancillary studies in cases in which diagnostic tissue fragments are mostly present on the smeared slides.

These limitations of ROSE could be minimised if microscopy of the sample could be conducted on viable cells, and if the assessed sample could eventually be recovered in suspension for triage.

Conventional transmitted light microscopy is not compatible with live cell imaging.[9] Therefore, we evaluated fluorescence microscopy techniques because fluorescence staining allows imaging of unfixed living cells,[9] and it has the advantage of allowing rapid one-step staining. Fluorescent images can be easily digitally converted to an image very closely resembling haematoxylin and eosin (H&E) staining.[9] Thus, fluorescence imaging techniques can allow cytologists to use their existing expertise in diagnosis. Several fluorescence microscopy techniques could theoretically allow an H&E-like image to be obtained from unfixed tissue particles. Fluorescent optical sectioning technologies[10] such as confocal or two-photon microscopies are suitable for high resolution imaging of multi-cell layer tissue fragments. However, due to their high expense and lack of portability, they are impractical for laboratories that may need to have ROSE performed in multiple locations. Simple epifluorescence microscopy is widely available and is inexpensive. However, image resolution is compromised by out-of-plane signals that progressively add glare, decreasing contrast and resolution from a plane of interest, especially when dealing with multi-cell layer tissue fragments.[11]

Deconvolution microscopy, also known as computational optical sectioning microscopy (COSM), is an image processing technique used to remove the light that comes from above or below a plane of interest when using simple epifluorescence microscopy.[12] The out-of-focus light degrades the image and is particularly problematic when looking at thick clusters of cells. To perform deconvolution microscopy, images are obtained with a simple epifluorescent microscope at a series of defined planes (e.g., 1 micron intervals) through the full thickness of the sample. A point source of light has a definable intensity—called the point spread function—away from its plane. The point-spread function of the microscopy system is used to back-calculate the most likely contribution of all sources of light at each plane, allowing digital subtraction of a substantial part of the glare. Multiple commercial software platforms as well as open source algorithms are available for deconvolution,[13] making it relatively inexpensive to use.

In this study, we emulated key steps of ROSE on suspended particles in solution, using residual needle rinses from fine needle aspiration (FNA) specimens, and demonstrate that a deconvolution algorithm significantly improves image quality of FNA specimens compared to raw images acquired via epifluorescence microscopy, allowing frequent definitive diagnosis. Further, we showed that the imaged fragments can be recovered in suspension for triage after performing ROSE.

2 | MATERIAL AND METHODS

Institutional Review Board approval was granted for this study (Docket H10396). Residual material in ThinPrep vials (Hologic Corporation) vials from 14 FNA samples, previously diagnosed at UMass Memorial Medical Center, were selected by two individuals (HL and TS) to cover a variety of tissue types and diagnoses. The original FNA samples had all been collected into CytoRich™ Red (ThermoFisher Scientific), centrifuged and transferred to a ThinPrep vial before making a ThinPrep and a Cellient (Hologic Corporation) cell block.

One mL of the residual material of each case in PreservCyt® Solution (Hologic Corporation) was pipetted to include grossly visible tissue fragments. The study material was suspended in a total of 1.5 mL PreservCyt Solution and centrifuged at 252 *g* for 4 min and the supernatant was discarded. The tissue fragments were stained with 1 μg/mL solution of Hoechst 33342 (ThermoFisher Scientific) together with a 1:5000 dilution of the supplied 5000× stock of SYPRO Red protein stain (Catalogue S6653, ThermoFisher Scientific) for 3 minutes. Fragments were washed one time in Hanks balanced salt solution, resuspended in 500 μL of HBSS and transferred by pipette to 35 mm glass bottom cell culture dish (Cellvis) for image acquisition (Figure S1 in the Supporting Information).

Wide-field fluorescence microscope (GE Healthcare Deltavision Personal Deconvolution Microscope) with Cool SNAP HQ camera and softWoRx 5.5 software was used to acquire stack images of optical sections of tissue fragments. The sample was first examined by differential interference contrast microscopy and up to five groups of tissue fragments for each specimen were selected as representative of the final diagnosis by one of the two individuals who were aware of the final diagnosis (HL and TS). The fluorescent signals were recorded for Hoechst 33342 (excitation/emission: 350/435 nm) and for SYPRO Red (excitation/emission: 300–550/676 nm) through the thickness of the fragments at 1 μm intervals in the Z plane. The raw fluorescent images at each image plane were saved. The image stacks for each of the fluorochromes were then deconvolved using the softWoRx 5.5 software package, and a second set of deconvolved images was saved. Images were downloaded from DeltaVision using ImageJ2 (an iteration of the NIH ImageJ program) and its plugin (Deltavision Opener).[13] For both the raw (non-deconvolved) and deconvolved images, a pseudocolouring operation was performed to approximate an H&E appearance using the Hoechst fluorescence (DNA or chromatin stain) as a surrogate for haematoxylin, and the SyproTM Red stain (protein stain) as a surrogate for eosin.[9] The steps for the pseudocolouring were conducted in ImageJ2 and the LUT panel,[13] by first inverting the black and white images separately for each channel to have a white background. Images were then converted to red-green-blue colour mode. A blue-purple colour was assigned to pixels for Hoechst channel, and red-pink colour was assigned to the Sypro Red channel. The two channels for each plane were then added to have a single image. ImageJ2 was then used to string the whole image stack for either raw or deconvolved images into a movie, emulating focusing up and down. The steps of image acquisition and processing are illustrated in Figure S2.

In this study, two tasks were completed by five cytopathologists including four senior cytopathologists with more than 5 years of experience and one junior cytopathologist with less than 2 years of experience. Four of the five cytopathologists performing the image evaluation received no exposure or training prior to rendering a diagnosis on evaluating digital images that are acquired and processed using the methods described in this study. In the first task, five cytopathologists, blinded to the original diagnoses, were presented with the deconvolved optical section movie stacks of the 14 cases and together with demographics, clinical history, and specimen sources as shown in Table 1, and asked to give both a categorical and descriptive diagnosis. Four categories of diagnosis were used: I. Negative for malignant cells; II. Atypical cells are present; III. Suspicious for malignancy; IV. Positive for malignant cells. If category II or III was chosen, the reason(s) for lack of a definitive diagnosis were specified. In the second task, 6 pairs of deconvolved and non-deconvolved stack images were evaluated blindly by five cytopathologists to rate which image series was preferred. The total number of deconvolved series preferred by cytopathologists was compared with that of non-deconvolved images. Fisher exact test was used to compare proportions.

After imaging, the study sample was recovered with a plastic disposable pipette from the well of the imaging chamber and used to make a ThinPrep slide and/or a cell block by following the standard operation protocols of UMass Memorial Health Care Cytology Laboratory. The recovered material was evaluated to confirm the presence and proper selection of diagnostic tissue fragments for imaging and interpretation, and to determine if the ROSE procedure alters the conventional appearance of the fragments.

3 | RESULTS

In the first task, the 14 cases selected consist of four benign and ten malignant reference diagnoses (Table 1) and a total 70 of evaluations by five cytopathologists were generated. Compared to the reference diagnoses, accurate definitive diagnoses were rendered by participating cytopathologists in 45 (64%) of 70 total evaluations, whereas equivocal diagnoses (atypical or suspicious) were rendered in 21 (30%) of the 70. Two false negative (3%) and two false positive (3%) diagnoses were rendered (Table 1).

Equivocal diagnoses were more likely rendered in benign cases (8 out of 20, 40%) than in malignant cases (13 out of 50, 26%). Cases 13 and 14 accounted for 33% of total equivocal diagnoses (7/21). Limitations leading to equivocal diagnosis were described by participants as due to sampling limitation (9/21, 43%), suboptimal image quality (8/21, 38%), and need for ancillary study (4/21, 19%; Table 1 and Figure 1).

The reference diagnoses of the two false negative diagnoses (cases 6 and 9) were high-grade mucoepidermoid carcinoma of parotid gland and metastatic thyroid carcinoma of torso soft tissue. The two false positive diagnoses were made on one case, which was benign inflamed pancreatic tissue from a patient with tuberculous pancreatitis presenting with a pancreatic body mass. These four erroneous diagnoses were made by four out of five cytopathologists and were described by participants as due to case-specific difficulty, such as misinterpretation of malignant squamous cells as benign squamous cells in the mucoepidermoid carcinoma case, and specimen overrun by necrosis in the benign pancreatic case (Figure 1F,M). The necrosis has a somewhat unanticipated appearance in these pseudocoloured images which may also contribute to the errors (Figure 1M).

In the second task, the image quality of deconvolved images was blindly and independently compared by the five cytopathologists to non-deconvolved images for six pairs selected from four representative cases (Figure 2) and a total of 30 evaluations were generated. The deconvolved images were preferred by cytopathologists in 23 of the 30 image pairs. The non-deconvolved images were preferred in 5 pairs (23 vs 5, $P < 0.01$ Fisher exact test), and the quality of the deconvolved image was considered the same as that of the non-deconvolved image in two cases (Table 2).

The H&E slides of cell block and ThinPrep slides made from the recovered sample proved the proper selection of tissue fragments for image acquisition and interpretation, and they showed that fluorescent staining and image acquisition do not have an adverse effect on subsequent morphology for a final diagnosis. (Figure 1O,P).

TABLE 1 Summary of the cases and evaluation results

Case No.	Age (year)	Gender	Source	Clinical history	History given to cytopathologists	Reference diagnosis	No. of diagnosis for each category[a]				Reason for non-definitive diagnosis
							I	II	III	IV	
1	50	M	Station 7 lymph node	Lung nodule	Lung nodule	Benign lymph node	5				
2	60	F	Axillary lymph node	Breast mass	Breast mass	Adenocarcinoma of breast origin				5	
3	75	M	Breast	Abnormal finding on CT scan	Abnormal CT	Adenocarcinoma of breast primary		3		2	Poor image quality, ancillary study needed
4	64	F	Supraclavicular lymph node	Malignant neuroendocrine tumour	Lymphadenopathy	Neuroendocrine carcinoma		1		4	Poor image quality
5	59	M	Inguinal lymph node	Squamous cell carcinoma of lung	Lymphadenopathy	Squamous cell carcinoma				5	
6	55	M	Parotid gland	Mucoepidermoid carcinoma	Parotid gland mass	Mucoepidermoid carcinoma	1[b]	3		1	Poor image quality
7	75	M	Station 7 lymph node	Mediastinal lymphadenopathy	Lymphadenopathy	Small cell carcinoma		3		2	Poor image quality, ancillary study needed
8	55	M	Neck	Malignancy of tongue base and neck mass	Neck mass	Squamous cell carcinoma				5	
9	81	M	Back	Anaplastic thyroid carcinoma	Back mass	Thyroid carcinoma	1 [b]		1	3	Ancillary study needed
10	79	F	Pancreas head	Pancreatic head mass	Pancreatic head mass	Adenocarcinoma			2	3	Need more groups
11	79	M	Pancreas body	Pancreatic body mass	Pancreatic body mass	Adenocarcinoma				5	
12	62	F	Thyroid	Thyroid isthmus nodule	Thyroid nodule	Benign colloid nodule	4	1			Need more groups
13	58	M	Pancreas	Pancreatic body mass	Pancreatic body mass	Negative for malignant cells		3		2[c]	Poor image quality
14	57	F	Thyroid	Thyroid nodule	Thyroid nodule	Benign thyroid nodule	1	4			Need more groups

[a]Categories of diagnosis: I. Negative for malignant cells; II. Atypical cells present; III. Suspicious for malignancy; IV. Positive for malignant cells.

[b]False negative.

[c]False positive.

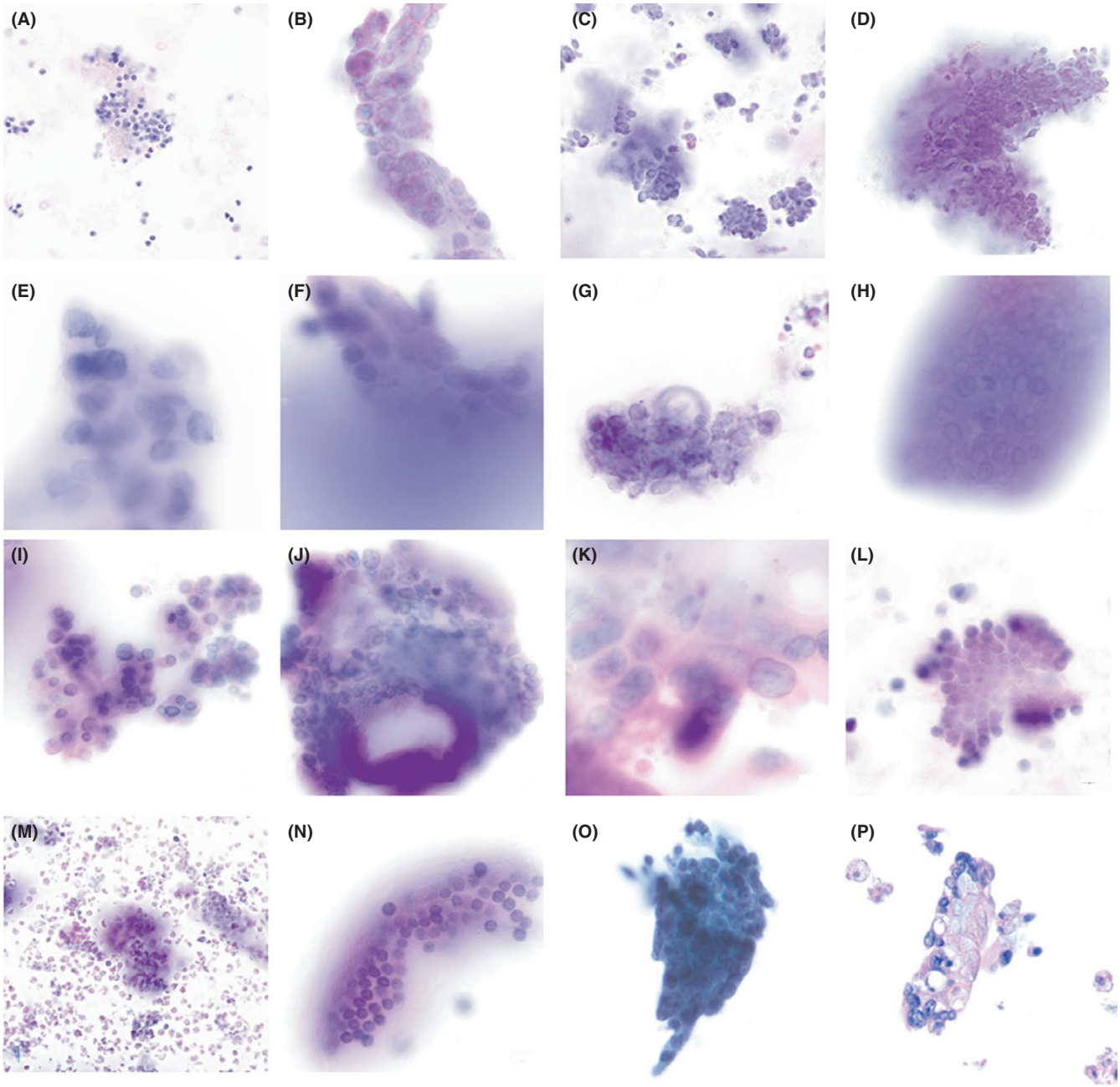

FIGURE 1 (A-N) Representative deconvoluted images from one plane of the 14 cases used in the study, in the order given in Table 1. (A) Case 1: Benign lymph node. (B) Case 2: Breast ductal carcinoma. (C) Case 3: Breast ductal carcinoma. (D) Case 4: Neuroendocrine carcinoma. (E) Case 5: Squamous cell carcinoma. (F) Case 6: Mucoepidermoid carcinoma. (G) Case 7: Small cell carcinoma. (H) Case 8: Squamous cell carcinoma. (I) Case 9: Thyroid carcinoma. (J) Case 10: Adenocarcinoma. (K) Case 11: Adenocarcinoma. (L) Case 12: Benign colloid nodule. (M) Case 13: Benign pancreatic tissue. (N) Case 14: Benign thyroid nodule. (O) ThinPrep of adenocarcinoma made from the recovered sample (case 11, panel K). (P) Cell block section of the original sample (case 11, panel K). (Pseudocolour [A-N]; Papanicolaou [O]; haematoxylin-eosin [P]; original magnifications ×200 [A-D,M] and ×400 [E-L,O-P])

4 | DISCUSSION

The advantage of cytology (less invasive, lower risk, potentially faster diagnosis) is offset by its lower definitive diagnosis rate compared to traditional core needle or excision biopsies.[14] The reasons for the lower definitive diagnostic rate are multi-fold, but they can probably mostly be attributed to technical problems[1]: poor performance of microbiopsy devices and difficulties in specimen handling are probably as important as the difficulty cytologists face in interpreting fewer or smaller fragments. Nevertheless, cytology is the best or even the only choice for making a diagnosis in certain clinical scenarios, such as ultrasound-guided endoscopic biopsy, or biopsy next to vital structures.

ROSE is needed to maximise the diagnostic performance of cytology.[1-4] Optimal specimen triage during ROSE becomes especially challenging when material is scant. Two of the major technical

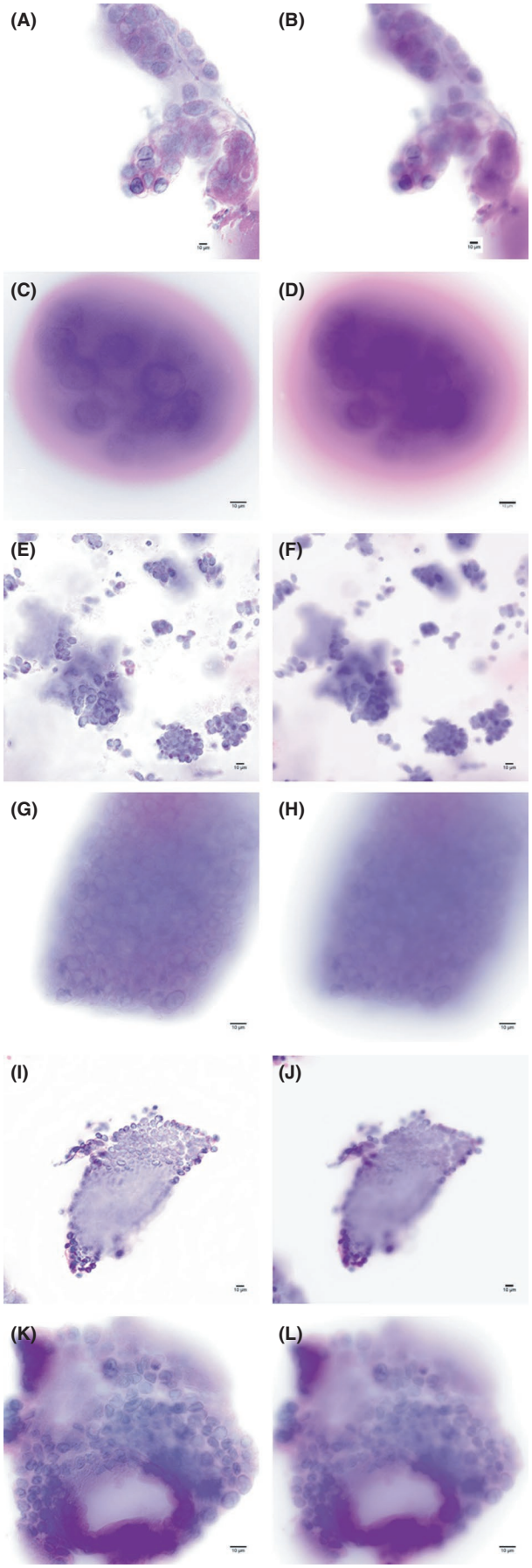

FIGURE 2 Comparison of deconvolved (left column) and non-deconvolved (right column) images at the same plane. (A-D) Case 2: Breast carcinoma. (E,F) Case 3: Breast carcinoma. (G,H) Case 8: Squamous cell carcinoma. (I-L) Case 10: Adenocarcinoma of pancreas. (Pseudocolour; original magnifications ×200 [A,B,E,F,I,J] and ×400 [C,D,G,H,K,L)

challenges of ROSE are to rapidly produce a proper representation of the FNA pass, and to have a sense of how much material was NOT examined and is available in the needle rinse for ancillary tests. An overly thick or overly thin smear, and a poorly preserved or stained smear can all waste precious material.

We propose that examination of an unfixed sample at the bedside as it is being collected offers solutions to the major problems for ROSE.

Confocal microscopy is a common method used in research for optical sectional microscopy and provides high resolution images of tissue fragments, typically to a depth of up to about 30 microns.[9] Two-photon microscopy is able to obtain a high resolution optical section even deeper into tissue—perhaps up to 50 microns.[9] However, confocal and especially two-photon microscopy may be impractically expensive to enable ROSE. No publications have used confocal or two-photon microscopies for ROSE of cytology specimens, though there is considerable interest in advanced microscopy techniques for the ex-vivo evaluation of surgical biopsies.[15-17]

Wide-field fluorescence microscopy, such as epifluorescence microscopy, is widely available in most clinical laboratories and allows rapid evaluation of specimens with one-step fluorescence staining. For certain well-defined applications, wide-field epifluorescence microscopy without deconvolution may be sufficient as a platform for ROSE.[18] The limitation of conventional epifluorescent microscopy is the drastic deterioration of image quality when fragment thickness exceeds one cell layer (about 10 microns).

Deconvolution microscopy can be used with wide-field fluorescence microscopy and has gained acceptance as an alternative to confocal and two-photon fluorescence microscopy.[11] This technology improves the image quality significantly for relatively thin objects.[12] The deconvolution algorithms, which now include open source programs, attempt to back-calculate the contribution of light from point sources above and below a plane of detection. To work, deconvolution theoretically requires that true negative (black) voxels be detectable, and this is not feasible when fluorescence emission takes place multiple planes above and below the plane of interest. Image deterioration from lack of contrast is evident in the sample set of the present study: The clearest images are in thinner portions of tissue, or from samples in which fluorescence signals are loosely packed above and below the plane. From the present study, resolution of chromatin detail is severely limited in fragments greater than about 30 microns. Still, this is an improvement over non-deconvolved images of small tissue fragments. Three-dimensional architecture was readily appreciated on stacks of deconvolved optical slices, akin to focusing up and down, allowing follicular architecture to be

discerned (Figure 3). In 30 comparisons (six samples compared by five cytopathologists), the deconvolved images were preferred in 23 comparisons while the non-deconvolved images preferred in five comparisons ($P < 0.01$). The image quality was considered the same in two comparisons. Relatively small fragments benefit the most from deconvolution.

We assessed the ability of the deconvolution platform to allow a definitive diagnosis, based on 14 cases from a variety of tissue types and diagnoses. Four of the five cytopathologists had no special training or experience with the type of imaging used. Deconvolution microscopy showed a sensitivity of 70% and specificity of 55% compared to the reference diagnosis if all equivocal diagnoses were considered as wrong diagnoses. It is worth pointing out that all the samples used in this study were adequate and we were focused on assessing whether this method allows cytopathologists to make definitive and accurate diagnosis instead of adequacy evaluation. The tissue fragments that were imaged and evaluated in this study were highly selected by individuals who knew the final diagnosis and the selection was to ensure the presence of diagnostic material. In real circumstances without knowing the diagnosis, a significantly greater amount of tissue would be selected for imaging and evaluation. While the sensitivity and the specificity might seem low for any diagnostic tools, this is actually a high bar to impose on ROSE: Generally, all that is needed for

TABLE 2 Summary of image quality comparison of deconvolved and non-deconvolved images in correspondence to Figure 2

Corresponding panel in Figure 2	Number of evaluations preferring deconvolved image	Number of evaluations preferring non-deconvolved image	Number of evaluations with no preference
A and B	3	2	0
C and D	4	1	0
E and F	5	0	0
G and H	4	0	1
I and J	3	2	0
K and L	4	0	1
In total	23	5	2

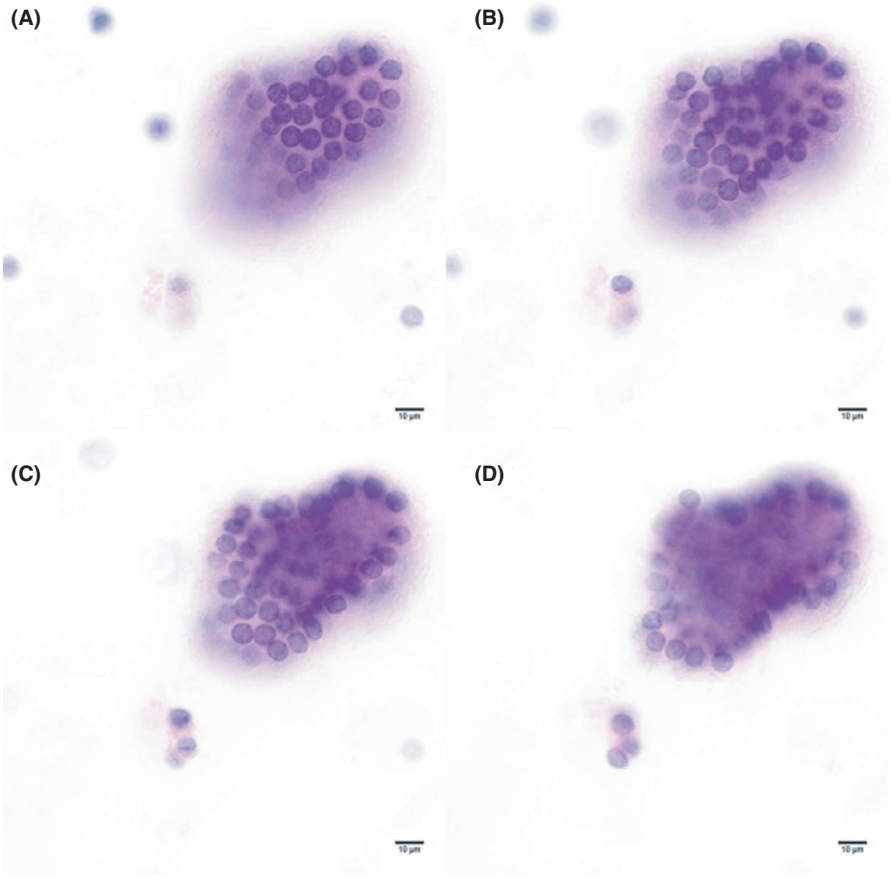

FIGURE 3 (A-D) Optical sections at 5 micron intervals through a thyroid follicle (case 14: Benign thyroid follicle; pseudocolour, 400×)

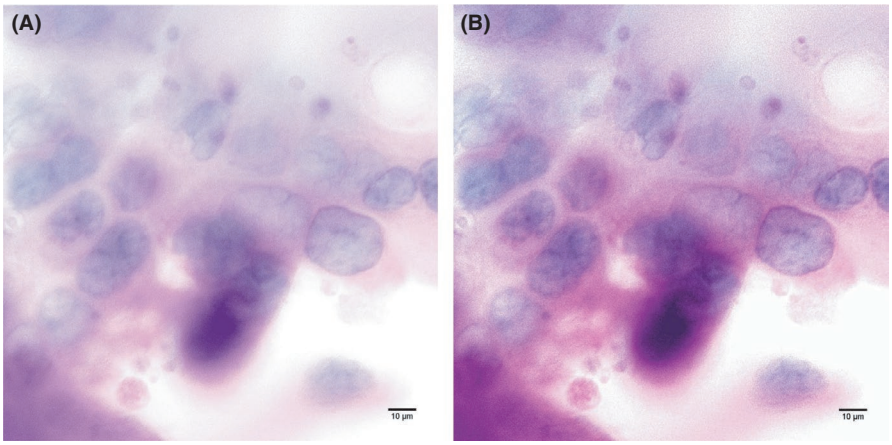

FIGURE 4 An example of further improvement of image quality using image adjustment functionality of Photoshop. (A) Deconvolved image without image adjustment. (B) Adjusted deconvolved image using HDR toning functionality of Photoshop

ROSE (all that is reimbursed by payers) is a statement of whether diagnostic material has been obtained or not. Additional studies with blinded selection of tissue fragments should be conducted for further evaluation of this technology.

In addition, amongst the 21 evaluations with equivocal diagnosis, 43% were due to sampling limitation. Considering only two to four image stacks were provided for each case in this study, a significant reduction of equivocal diagnosis can be achieved by evaluating more image stacks for future studies. Therefore, we believe our results establish the feasibility of using deconvolution microscopy for ROSE.

While we demonstrated that deconvolution microscopy significantly improved the Z stack image quality of tissue fragments, many techniques are available to further improve the image quality and therefore image interpretability, such as using the image adjustment functionalities in Photoshop (Figure 4).

Turn-around-time would be a major concern when evaluating any method or technology used for ROSE. In this study, the key steps from sample preparation to evaluation include fluorescent staining, sample loading, image acquisition and image processing. It takes approximately 11–15 minutes to prepare the specimen for imaging; image acquisition takes 30 seconds to 1 minute for each tissue fragment depending on the thickness of tissue fragments. The entire process for each case takes approximately 30 minutes. However, the manner of handling the sample can be streamlined, accelerated, and probably fully automated, allowing ROSE via telepathology without the need for a technical person to prepare smears and stain slides. For this study, we made up a manual process for getting material to an optical plane for deconvolution microscopy. We also chose to rinse the excess dye, to reduce background. However, the fluorescence of Hoechst 33342 and other DNA binding dyes is so much stronger when it is bound that protocols for visualising fluorescent DNA binding dyes do not mandate a washing step.[19] Since most cytopathologists are familiar with H&E staining, we developed a pseudocolouring algorithm, using ImageJ and its open source plugins. These image manipulations take seconds and can easily be automated. It is likely that a needle rinse could ultimately be examined within about 5 minutes of collection with this technology.

We used fixed archival material for this study. However, a number of fluorochromes can penetrate living cells, including Hoechst 33342 and fluorescein (which emulates eosin staining of proteins). Image stacks can be obtained and processed using the same methods described in this study. Thus, we believe the basic concept can be adapted to evaluate living tissue fragments/cells in suspension.

After staining, cells embedded for a cellblock or for a ThinPrep showed no morphological alteration. Residual fluorochrome from the ROSE procedure could pose a problem for flow cytometry, but two solutions can be anticipated. First, only part of the sample (for example a random sample of the suspension) could be used for the ROSE, the part that would ultimately be converted to a monolayer preparation or cellblock. Second, if only a DNA stain were used, a single fluorochrome could be used and it could be chosen to not overlap with the needed fluorescent channels for flow cytometry.

We envision that the clinician can simply rinse the needle in a container adapted to hold part of the sample at an optical plane, enabling deconvolution microscopy to capture electronically transmissible images through a representative part of the sample within minutes. This technology could assess the quality and quantity of the entire material obtained during a ROSE procedure. After the ROSE procedure, the entire sample, or parts of it, could then specifically be triaged for necessary ancillary studies.

In conclusion, our study, as a proof of concept, demonstrates that deconvolution fluorescence microscopy improves image quality and allows frequent definitive diagnosis. With further improvement and optimisation, deconvolution microscopy shows promise for facilitating ROSE.

ACKNOWLEDGEMENTS

None.

CONFLICT OF INTEREST

No conflict of interest declared.

AUTHOR CONTRIBUTIONS

Haihui Liao contributed to conception, design, acquisition, analysis and interpretation; drafted the manuscript, critically revised the manuscript, and gave final approval; and agrees to be accountable for all aspects of work ensuring integrity and accuracy. Todd

Sheridan contributed to conception, design, acquisition, analysis and interpretation. Ediz Cosar, Christopher Owens, Tao Zuo, Xiaofei Wang, Ali Akalin, and Dina Kandil contributed to acquisition and analysis. Karen Dresser, Kevin Fogarty, Karl Bellve, and Christina Baer contributed to acquisition. Andrew Fischer contributed to conception, design, acquisition, analysis, and interpretation, and drafted the manuscript.

DATA AVAILABILITY STATEMENT

The data that support the findings of this study are available from the corresponding author upon reasonable request.

ORCID

Haihui Liao https://orcid.org/0000-0002-0098-4682

REFERENCES

1. Fischer AH. New quantitative data on cell blocks. *J Am Soc Cytopathol*. 2019;8(2):49-51.
2. Schmidt RL, Witt BL, Lopez-Calderon LE, Layfield LJ. The influence of rapid onsite evaluation on the adequacy rate of fine-needle aspiration cytology: a systematic review and meta-analysis. *Am J Clin Pathol*. 2013;139(3):300-308.
3. Matynia AP, Schmidt RL, Barraza G, Layfield LJ, Siddiqui AA, Adler DG. Impact of rapid on-site evaluation on the adequacy of endoscopic-ultrasound guided fine-needle aspiration of solid pancreatic lesions: a systematic review and meta-analysis. *J Gastroenterol Hepatol*. 2014;29(4):697-705.
4. Fung AD, Collins JA, Campassi C, Ioffe OB, Staats PN. Performance characteristics of ultrasound-guided fine-needle aspiration of axillary lymph nodes for metastatic breast cancer employing rapid on-site evaluation of adequacy: analysis of 136 cases and review of the literature. *Cancer Cytopathol*. 2014;122(4):282-291.
5. Marshall AE, Cramer HM, Wu HH. The usefulness of the cell transfer technique for immunocytochemistry of fine-needle aspirates. *Cancer Cytopathol*. 2014;122(12):898-902.
6. Fischer AH, Hutchinson LM. Technical and US regulatory issues in triaging material for the molecular laboratory. *Cancer Cytopathol*. 2017;125(2):83-90.
7. Saqi A. The state of cell blocks and ancillary testing: past, present, and future. *Arch Pathol Lab Med*. 2016;140(12):1318-1322.
8. Fischer AH, Schwartz MR, Moriarty AT, et al. Immunohistochemistry practices of cytopathology laboratories: a survey of participants in the College of American Pathologists Nongynecologic Cytopathology Education Program. *Arch Pathol Lab Med*. 2014;138(9):1167-1172.
9. Schmolze DB, Standley C, Fogarty KE, Fischer AH. Advances in microscopy techniques. *Arch Pathol Lab Med*. 2011;135(2):255-263.
10. Conchello JA, Lichtman JW. Optical sectioning microscopy. *Nat Methods*. 2005;2(12):920-931.
11. Webb DJ, Brown CM. Epi-fluorescence microscopy. *Methods Mol Biol*. 2013;931:29-59.
12. Biggs DSC. A practical guide to deconvolution of fluorescence microscope imagery. *Microscopy Today*. 2010;18(1):10-14.
13. Rueden CT, Schindelin J, Hiner MC, et al. ImageJ2: ImageJ for the next generation of scientific image data. *BMC Bioinformatics*. 2017;18(1):529.
14. Khoury T, Sbeit W, Ludvik N, et al. Concise review on the comparative efficacy of endoscopic ultrasound-guided fine-needle aspiration vs core biopsy in pancreatic masses, upper and lower gastrointestinal submucosal tumors. *World J Gastrointest Endosc*. 2018;10(10):267-273.
15. Krishnamurthy S, Cortes A, Lopez M, et al. Ex vivo confocal fluorescence microscopy for rapid evaluation of tissues in surgical pathology practice. *Arch Pathol Lab Med*. 2018;142(3):396-401.
16. Reder NP, Glaser AK, McCarty EF, Chen Y, True LD, Liu JTC. Open-top light-sheet microscopy image atlas of prostate core needle biopsies. *Arch Pathol Lab Med*. 2019;143(9):1069-1075. doi:10.5858/arpa.2018-0466-OA
17. Levenson RM, Fereidouni F. MUSE: a new, fast, simple microscopy method for slide-free histology and surface topography. *FASEB J*. 2016;30(1_Supplement):51.3.
18. Schmolze DB, Fischer AH. An automatable method for determining adequacy of thyroid fine-needle aspiration samples. *Arch Pathol Lab Med*. 2019;143(9):1084-1088.
19. Allan RW, Ansari-Lari MA, Jordan S. DRAQ5-based, no-lyse, no-wash bone marrow aspirate evaluation by flow cytometry. *Am J Clin Pathol*. 2008;129(5):706-713.

SUPPORTING INFORMATION

Additional supporting information may be found in the online version of the article at the publisher's website.

How to cite this article: Liao H, Sheridan T, Cosar E, et al. Deconvolution microscopy: A platform for rapid on-site evaluation of fine needle aspiration specimens that enables recovery of the sample. *Cytopathology*. 2022;33:312–320. doi:10.1111/cyt.13106